

Positronium localization in solid and liquid methane

This article has been downloaded from IOPscience. Please scroll down to see the full text article.

1991 J. Phys.: Condens. Matter 3 2167

(<http://iopscience.iop.org/0953-8984/3/13/019>)

View [the table of contents for this issue](#), or go to the [journal homepage](#) for more

Download details:

IP Address: 171.66.16.151

The article was downloaded on 11/05/2010 at 07:10

Please note that [terms and conditions apply](#).

Positronium localization in solid and liquid methane

S J Wang[†], H Nakanishi[‡] and Y C Jean[‡]

[†] Department of Physics, Wuhan University, Wuhan, People's Republic of China

[‡] Department of Chemistry, University of Missouri–Kansas City, Kansas City, MO 64110, USA

Received 20 March 1990, in final form 23 November 1990

Abstract. Positron lifetimes and Doppler broadening of annihilation radiations have been measured on high-purity condensed methane at temperatures ranging from 30 K to 150 K. In the solid phase, the o-Ps lifetime and S parameter increase sigmoidally as a function of temperature. This variation is interpreted as being due to a Ps atom being trapped in thermally activated vacancy-type defects. A vacancy formation enthalpy of 0.10 ± 0.02 eV is obtained in solid methane. In the liquid phase, large values for the o-Ps lifetime and intensity, and a strong temperature variation of these values are observed. These results are interpreted as being due to the localization of the Ps atom in a bubble state. The temperature dependence of Ps bubble size and microscopic surface tension are evaluated using o-Ps lifetime data.

1. Introduction

The study of Positronium (Ps) formation and localization in molecular solids and liquids has been a special area of interest in the research field of positron annihilation spectroscopy (PAS) in the last decade [1–3]. This may be due to the fact that there is a high probability of Ps atom formation and the formation and annihilation characteristics of Ps in a molecular system depend on the chemical and physical properties of the molecular substances under study.

The detection of point defects in metals using PAS has been known of for more than twenty years [4], but the investigation of defect properties in molecular materials has only been developed in recent years. The reasons are perhaps the difficulty in obtaining molecular samples which are nearly impurity-free, and the complex Ps molecule interactions. The success of using PAS as a defect tool in molecular solids relies on the recent discovery of Ps trapping in defects, such as in ice and plastic crystals [5, 6]. In molecular solids one can obtain information about defect properties by measuring the positronium lifetimes and Doppler broadening of the annihilation radiations in a controlled system by varying, for example, temperature or external radiation [7].

In molecular liquids, the Ps atom is found to be localized in a microscopic cavity, called a Ps bubble, which is created by an induced local potential between the Ps and the liquid. The bubble model was first suggested by Ferrell [8] to explain an unexpectedly long o-Ps lifetime in liquid helium, and was later developed by Roelling *et al* [9].

Methane is a classical molecule for structural study. It has the strongest C–H bond among the saturated hydrocarbons and possesses a unique symmetrical structure. Both theoretical and experimental investigations on solid and liquid methane have been

carried out extensively in other fields of research, such as those of muons [10] and neutrons [11]. In the present work, we use positron lifetime and Doppler broadening to study the Ps formation and annihilation in methane over a wide temperature range (30–150 K) and report some new structural information: phase transition, vacancy formation enthalpy, Ps bubble size and microscopic surface tension.

2. Experimental methods

2.1. Sample preparation

The research grade methane gas (99.99% purity from Matheson gas, NJ) was first passed through an oxygen purifier to reduce oxygen and other impurities to less than 1 ppm and then condensed in a sample cell made of aluminium which was attached to a He refrigerator at a temperature of 30 K. The sample cell was mounted on a cool head of a closed-cycle He refrigerator (Air Product Displex) with a temperature control better than ± 0.1 K over a temperature range from 10 K to 300 K. A stainless-steel gas-handling line was employed to manipulate the gas condensation. The gas line and sample cell were leak checked under a high vacuum ($<10^{-5}$ Torr). The sample cell volume was 1 cm^3 . The amount of methane gas condensed in the cell was controlled and calculated from the volume and pressure of the gas-handling line according to the ideal gas law. After methane was condensed, the sample was annealed at 65 K for 48 h, and then the temperature was decreased gradually (5 K h^{-1}) to 30 K to start temperature dependent experiments.

2.2. Positron annihilation spectroscopy

A $30 \mu\text{Ci}^{22}\text{Na}$ positron source, which was sealed between two aluminium foils of thickness 0.8 mg cm^{-2} , and positioned at the centre of the sample cell, was used in the experiments. The positron lifetime measurements were performed using a conventional fast-fast coincident system. The time resolution of the system was determined to be 280 ps from the prompt curve of a ^{60}Co source. Each positron lifetime spectrum contained about 5×10^5 events. The obtained lifetime spectra were analysed using the PATFIT computer program [12]. The Doppler broadening energy spectra of annihilation radiations were measured using a coaxial Ge(Li) detector (15% efficiency) with 1.5 keV resolution measured at 497 keV (^{103}Ru peak). The results of Doppler broadening measurements were expressed as an S parameter which was taken to be the ratio of the total count in the central region of the 511 keV (± 0.9 keV) peak to the total count over the whole spectrum where the background has been subtracted.

3. Results and discussions

We have measured the positron lifetime spectra in condensed methane as a function of temperature from 30 K to 150 K. Three positron lifetimes were resolved for the spectra. The short component ($\tau_1 = 0.12 \text{ ns}$), the intermediate component ($\tau_2 = 0.33\text{--}0.44 \text{ ns}$), and the long component ($\tau_3 = 2.3\text{--}7.3 \text{ ns}$) are assigned due to para-positronium (p-Ps)

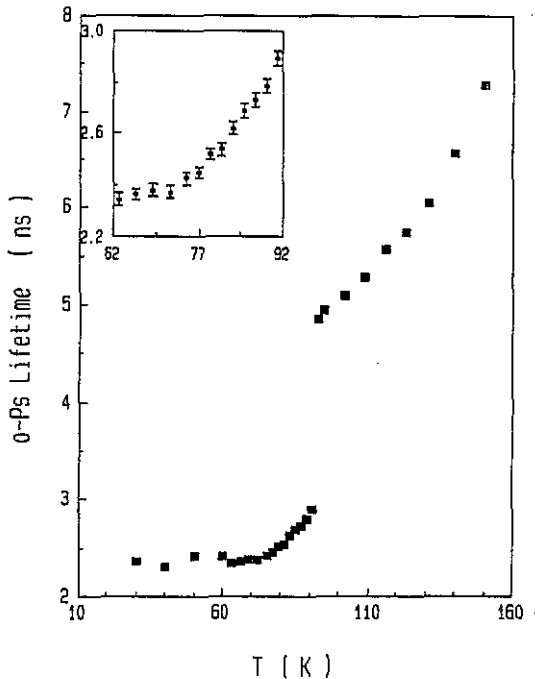


Figure 1. The variation of o-Ps lifetime (τ_3) with temperature in condensed methane.

annihilation, positron (not forming Ps) annihilation and o-Ps annihilation, respectively. The results of o-Ps lifetime τ_3 , positron lifetime τ_2 and their corresponding intensities I_3 and I_2 are shown in figures 1–3. The S parameter result as a function of temperature is shown in figure 4. Since o-Ps is particularly sensitive to the properties of a molecular system, our discussions emphasize the variations of τ_3 , I_3 and S with respect to temperature.

3.1. Solid methane

The phase transformation from solid to liquid methane was clearly seen at 91.0 ± 0.5 K ($T_c = 90.66$ K for methane [13]) in figures 1–3 where abrupt jumps are observed for o-Ps lifetime τ_3 (2.9 ns–5.0 ns), o-Ps intensity I_3 (20%–27%) and positron intensity I_2 (32%–24%). The large values of τ_3 , I_3 and τ_2 are observed in liquid methane. The fact that the o-Ps lifetime and its intensity in the liquid phase are much higher than in the solid phase infers that the Ps formation mechanism and annihilation rate in solid methane are different from those in liquid methane.

After Ps is formed in solid methane two states may result before annihilation occurs: a delocalized state in the bulk, and a localized state in the defect. The variations of o-Ps lifetime at temperatures between 62 K and 92 K (shown in the inserted plot of figure 1) show this two-state behaviour. Below 65 K, o-Ps lifetimes are nearly constant ($= 2.3$ ns), then increase sigmoidally with temperature from 65 K to 91 K. This variation is very similar to the positron lifetime variation in metals at temperatures above $0.7 T_m$ (T_m is melting temperature). As is well known, the Ps atom can be formed in the free volumes of molecular solids [14]. The large increase in o-Ps lifetime with temperature above 65 K

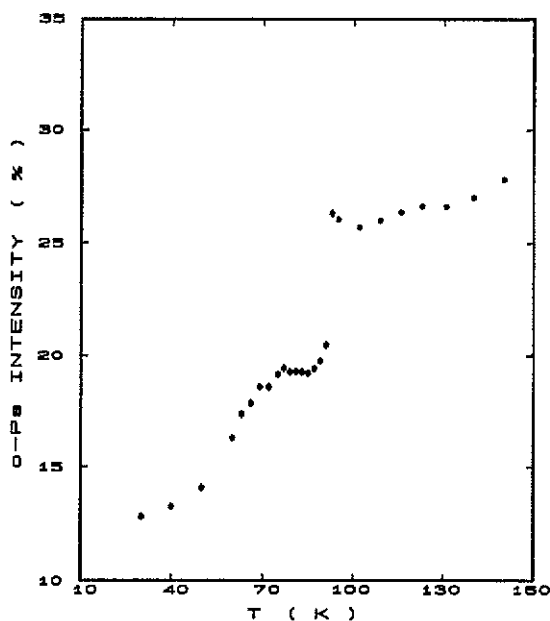


Figure 2. The variation of o-Ps intensity (I_3) with temperature in condensed methane.

is expected to be due to Ps trapping in defects, which can be described by the free volume model. This is similar to that for ice [5]. The density of solid methane is 0.45 g cm^{-3} and its thermal expansion volume is relatively large. According to the universal correlation between o-Ps lifetime and void volume in molecular solids [1], the lifetimes of 2.3 ns (65 K) and 2.9 ns (91 K) correspond to volumes 100 \AA^3 and 200 \AA^3 respectively. The 100% volume increase is much more than the thermal expansion of only a few percent in solid methane in the temperature range 65 K–91 K. Since the thermal expansion volume cannot account for this large lifetime change, a good explanation is that the Ps atom is localized in defects. The best candidates for the localized sites are thermally generated vacancy-type defects. According to the Ps trapping model in a molecular solid [5], the lifetime spectra can be analysed as four components with two o-Ps components. In this work, we found that three-lifetime analysis gives a more stable and consistent result. Since the o-Ps intensity, shown in figure 2, is nearly constant between 70 K and 90 K, our o-Ps lifetime shown in figure 1 is an average o-Ps lifetime from two o-Ps states, i.e. localized and delocalized. Using an equation analogy to the two-states trapping model derived from metallic systems [4], we use the following equation to express the temperature variation of the o-Ps lifetime, τ :

$$(\tau - \tau_b)/(\tau_d - \tau) = A \exp(-E_a/kT) \quad (1)$$

where A is a constant and k is Boltzmann's constant, E_a is the defect formation enthalpy, τ_b and τ_d are the o-Ps lifetimes in the bulk and at the vacancy-type defect respectively. With $\tau_b = 2.35 \text{ ns}$ and $\tau_d = 2.90 \text{ ns}$, the Arrhenius plot is shown in figure 5(a). From the slope of the plot in this figure a defect formation enthalpy of $0.10 \pm 0.02 \text{ eV}$ is obtained. This value agrees well with the reported value of 9.2 kJ mol^{-1} [15] for solid methane.

The Ps atom trapping in vacancy-type defects in solid methane is further confirmed by Doppler broadening measurements. The results for the S parameter are shown in

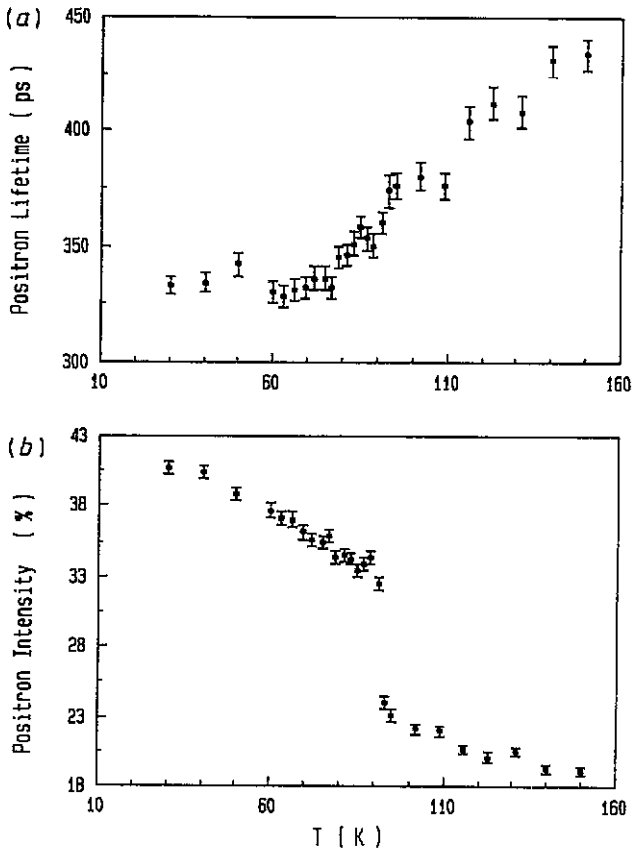


Figure 3. The positron lifetime (τ_2) (a) and positron intensity (I_2) (b) against temperature in condensed methane.

figure 4. The phase transformation from solid to liquid and the transition temperature can be observed from the inflection point of the curve at 91 ± 1 K, which coincides with the melting point of methane. The typical sigmoidal shape of the S parameter variations with temperature from 30 K to 110 K also indicates a thermally activated process for vacancy formation. Using the same trapping model as described above, we express the temperature variation of the S parameter by the following equation:

$$(S - S_b)/(S_d - S) = A \exp(-E_a/kT) \quad (2)$$

where S_b and S_d are values of the S parameter in the bulk and the vacancy-type defect, respectively. From the Arrhenius plot shown in figure 5(b), a defect formation enthalpy $E_a = 0.10 \pm 0.02$ eV was obtained. This result agrees with that obtained from lifetime data.

3.2. Liquid methane

In liquids, the positronium is believed to exist at a self-trapping state. Both existing theoretical and experimental investigations support the model of positronium bubble in

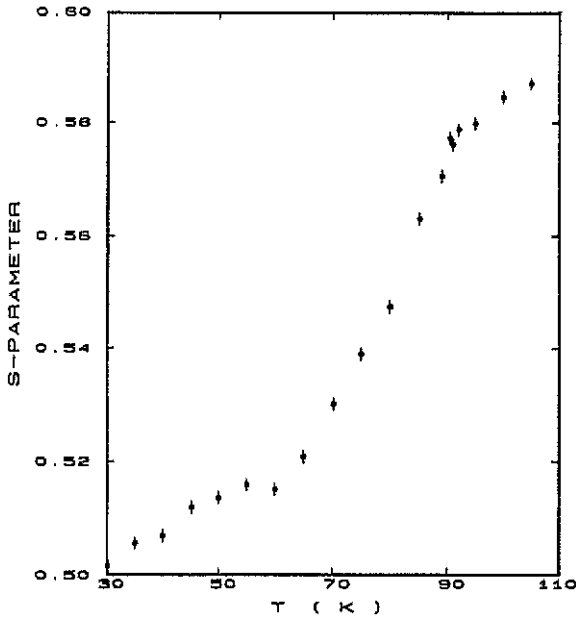


Figure 4. The S parameter of Doppler broadening against temperature in condensed methane.

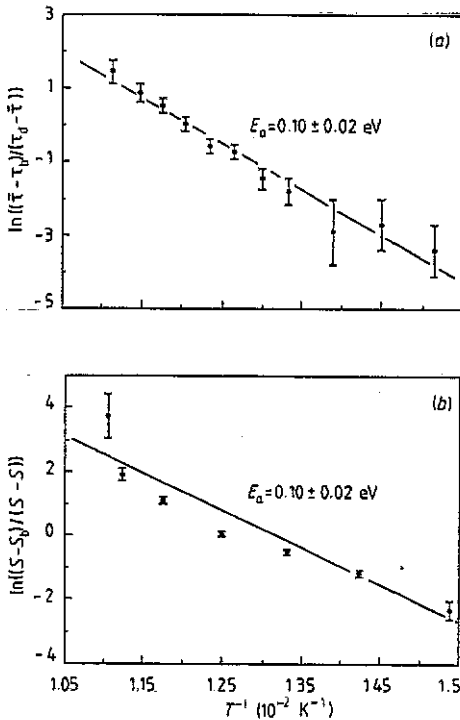


Figure 5. The Arrhenius plots of o-Ps lifetime (a) and S parameter (b) against the inverse absolute temperature for solid methane. The defect formation energy $E_a = 0.10 \pm 0.02 \text{ eV}$ was obtained from the slopes of both plots.

liquid. A Ps bubble is created as a result of the repulsive force between the electron of Ps and electrons of the medium. Thus, from the observed Ps annihilation characteristics, physical properties of liquids, such as surface tension, viscosity, bubble size, dielectric constant, etc. can be obtained.

As shown in figure 1, the o-Ps lifetime and its intensity have an onset at the solid-liquid transition (91 K) and the o-Ps lifetime varies more with temperature for liquid methane (93 K–150 K) than for the solid phase (below 91 K). This supports the Ps bubble formation in liquid methane. A high Ps formation probability is also observed in liquid methane as shown in figure 2.

Since the internal pressure created by the zero point energy of Ps in the bubble is counterbalanced by the contractual pressure due to the surface tension of the surrounding molecules, a correlation between o-Ps lifetime in the bubble and the surface tension is expected. Empirical relations between surface tensions γ and o-Ps pick-off annihilation rates λ_p , which are the inverse of o-Ps lifetime, have been reported by Tao [16] for *n*-alkanes: $\lambda_p = 0.061 \gamma^{0.50}$ and for oxygenated short-chain hydrocarbons: $\lambda_p = 0.046 \gamma^{0.55}$. Subsequently the bubble size and surface tension can be evaluated. By minimizing the total energy of the Ps atom in a bubble:

$$dE/dR + d(4\pi R^2\gamma)/dR = 0 \quad (3)$$

one obtains the following equation [17]

$$\gamma = \hbar^2 K^3 / 16\pi m R (KR - \tan KR) \quad (4)$$

where R is the bubble radius, m is the electron mass, γ is the surface tension and $K = \sqrt{4mE}/\hbar$ is the Ps wave vector. K and R are estimated from the quantum mechanical probability of the Ps wavefunction outside the potential well and from the assumption that the Ps annihilation rate is given by the Dirac annihilation rate equation. In this paper we adopted a semi-empirical method [2] to estimate the bubble radius R without knowing Z_{off} . This method approximates Ps in a bubble to a particle in an infinite spherical potential of radius R_0 with an electron layer of thickness ΔR as originally used by Tao [16] and Eldrup *et al* [18]. The relation between the o-Ps annihilation rate, $\lambda_p(\tau_3^{-1})$, and the bubble radius, R (in Å), is given [2] by

$$\lambda_p = 2[1 - R/R_0 + (1/2\pi) \sin(2\pi R/R_0)] \quad (5)$$

where $R_0 = R + \Delta R$. By fitting the measured o-Ps lifetimes and the known hole sizes for molecular solids [18] and zeolites [19], a best value of $\Delta R = 1.66$ Å [2] was obtained. From equations (4) and (5), and measured o-Ps annihilation rates in liquid methane (93 K–150 K), the bubble radius and microscopic surface tension can be evaluated. The results are shown in table 1 along with other physical parameters. Since the Ps wave vector K or the ground state energy E estimated from this method is always higher than that from the finite potential, the obtained surface tension value may be considered to be an upper limit.

4. Conclusion

Positron lifetime and Doppler broadening measurements have been studied on high-purity condensed methane as a function of temperature between 30 K and 150 K. For solid methane, the o-Ps lifetime and S parameter show strong temperature dependence

Table 1. The bubble radius (R) and surface tension (γ) for liquid methane calculated from the bubble model

T (K)	τ_3 (ns)	Density (g cm^{-3})	Pressure (Torr)	R (Å)	γ (dyn cm^{-1})
93	4.85 ± 0.04	0.4499	350	4.67	18.0
95	4.94 ± 0.04	0.4472	465	4.71	17.6
102	5.09 ± 0.04	0.4378	517	4.78	16.3
109	5.29 ± 0.04	0.4280	724	4.87	15.1
116	5.57 ± 0.04	0.4180	1134	5.00	13.8
123	5.73 ± 0.03	0.4077	1758	5.07	12.5
131	6.04 ± 0.04	0.3951	2895	5.19	11.0
140	6.56 ± 0.04	0.3797	4705	5.40	9.4
150	7.28 ± 0.04	0.3611	7497	5.67	7.5

above 65 K. These variations were interpreted as o-Ps localization in a thermally generated defect. By invoking the Ps trapping model in a molecular solid, a vacancy formation energy $E_a = 0.10 \pm 0.02$ eV was obtained. For liquid methane, the o-Ps annihilation characteristics support the Ps bubble model. The bubble size and microscopic surface tension were estimated from lifetime results.

References

- [1] Eldrup M 1982 *Positron Annihilation* ed P G Coleman, S C Sharma and L M Diana (Amsterdam: North-Holland) p 753
- [2] Nakanishi H and Jean Y C 1988 *Positron and Positronium Chemistry* ed D M Schrader and Y C Jean (Amsterdam: Elsevier) p 159
- [3] Wang S J and Jean Y C 1988 *Positron and Positronium Chemistry* ed D M Schrader and Y C Jean (Amsterdam: Elsevier) p 255
- [4] For example, see 1983 *Positron Solid-State Physics* ed W Brandt and A Dupasquier (Amsterdam: North-Holland)
- [5] Eldrup M, Mogensen O and Trumphy G 1972 *J. Chem. Phys.* **57** 495
- [6] Eldrup M, Pedersen N J and Sherwood J N 1979 *Phys. Rev. Lett.* **43** 1407
- [7] Jean Y C and Ache H J 1978 *J. Phys. Chem.* **82** 656
- [8] Ferrell R A 1957 *Phys. Rev.* **108** 167
- [9] Roelling L O 1967 *Positron Annihilation* ed A T Stewart and L O Roelling (New York: Academic) p 127
- [10] Jean Y C, Stadlbauer J M and Ganti R L 1987 *J. Phys. Chem.* **91** 1270
- [11] Bloom M and Morrison J A 1973 *Surface and Defect Properties of Solids* (London: The Chemical Society) p 140
- [12] Kirkegard P, Eldrup M, Mogensen O and Pedersen N J 1981 *Comp. Phys. Commun.* **23** 307
- [13] For example see 1980 *Matheson Gas Data Book* 6th edn ed W Braker and A L Mossman (Bridgeport, NJ: Matheson Co.)
- [14] Brandt W, Berko S and Walker W W 1960 *Phys. Rev.* **120** 1289
- [15] Brooks A H 1974 *PhD Thesis* Canterbury University
- [16] Tao S J 1972 *J. Chem. Phys.* **56** 5499
- [17] Buchikhin A P, Goldanskii V I and Shantarovich V P 1971 *Sov. Phys.-JETP* **33** 615; 1971 *JETP Lett.* **13** 444
- [18] Eldrup M, Lightbody D and Sherwood J N 1981 *Chem. Phys.* **63** 51
- [19] Nakanishi H and Vjihira Y 1982 *J. Phys. Chem.* **86** 4446